AlGaAsSb-InGaAsSb-GaSb epitaxial heterostructures for uncooled infrared detectors

Oleg V. Sulima[a], Sarbajit Datta[a,b], Jeff A. Cox[a], Michael G. Mauk[a], Sir B. Rafol[c]
[a]AstroPower Inc., Solar Park, Newark, DE 19716
[b]University of Delaware, Electrical and Computer Engineering Department, Newark, DE 19716
[c]Jet Propulsion Laboratory, 4800 Oak Grove Drive, Pasadena, CA 91109
E-mail: sulima@astropower.com

Abstract

Lattice matched n-type AlGaAsSb-InGaAsSb-GaSb heterostructures for uncooled infrared detectors including separate absorption and multiplication avalanche photodiodes (SAM-APD) as well as low-voltage InGaAsSb APDs were grown using inexpensive liquid phase epitaxy. Formation of the pn-junction was performed through diffusion of Zn from the vapor phase. Responsivity at $\lambda = 2$ μm as high as 3.5 A/W was achieved in InGaAsSb APD biased at 8 V with the avalanche multiplication starting at 6 V. Our calculations have shown that the above parameters can result in a NEP value as low as $1x10^{-12}$ W or D* value as high as $2x10^{10}$ cm·Hz$^{1/2}$/W at room temperature for 400 μm diameter (200 μm diameter photoactive area) APD diodes.

Introduction

AlGaAsSb-InGaAsSb heterostructures lattice matched to GaSb are of great interest for use in high-performance photodetectors, LEDs and lasers in the mid-infrared wavelength region as well as for thermophotovoltaic devices. AstroPower has accumulated considerable experience in the development of inexpensive liquid phase epitaxy (LPE) for fabrication of AlGaAsSb-InGaAsSb photodetectors [1-3].

LPE inherently provides high material quality, both with respect to defect density and purity. This may be attributed to the preferential segregation of impurities to the liquid phase, the high mobility of atoms in the liquid phase (as compared to surface diffusion upon which vapor phase techniques depend), and near-equilibrium growth conditions.

In this work, we continued to study LPE growth of AlGaAsSb-InGaAsSb heterostructures. Additionally, a technically uncomplicated and productive method of Zn diffusion from the vapor phase was used to simplify and improve the fabrication technology of photodetectors including SAM-APDs and low-voltage APDs.

APDs are widely used for optical fiber communication. However, commercially available Si APDs require high voltage (several hundreds of Volts) that limits their application. In this work, low-voltage (6-8 Volts) APDs were developed. Moreover, in comparison with Si, the long wavelength sensitivity of the developed devices was extended to 2 μm.

0-7803-7478/02/$17.00 © 2002 IEEE

Experimental

Epitaxial growth

A standard horizontal slide boat technique is used for the LPE growth of the InGaAsSb and AlGaAsSb layers. The graphite slide boat is situated in a sealed quartz tube placed in a microprocessor-controlled, programmable, three-zone tube furnace. The growth ambient is palladium-diffused hydrogen at atmospheric pressure with a flow rate of 300 ml/min. The substrates with an area of 14x14 mm^2 are polished, (100) oriented, *n*-type GaSb wafers doped to 3-5 x 10^{17} cm^{-3} with tellurium.

The basic growth solution for InGaAsSb is indium (x_{In}=0.59), gallium (x_{Ga}=0.21) and antimony (x_{Sb}=0.20), where x_i is the atomic fraction of the element *i* in the solution. High purity (99.9999%) indium, gallium, and antimony metals are used and no intentional doping of the melt is applied. Prior to growth, the melt is baked out at 700 °C for 15 hours under flowing hydrogen to de-oxidize the metallic melt components and outgas residual impurities. After the baking and cooling, an undoped polycrystalline float InAs wafer is loaded on top of the melt, and the boat is heated again up to 530°C. Arsenic from the float InAs wafer is added to the melt through a partial dissolution of the wafer at this temperature. The melt is equilibrated for 1 hour at 530 °C and then cooled down to the growth temperature. At 515 °C, the substrate is contacted with the melt for 2 minutes to grow a 5 micron thick *n*-type $In_{0.15}Ga_{0.85}As_{0.17}Sb_{0.83}$ base layer with an electron concentration of 2-4x10^{16} cm^{-3}. Afterwards, the melt is wiped from the substrate. Electron probe microanalysis (EPMA) was used to determine the solid composition of the InGaAsSb layer. The electron concentration in InGaAsSb was calculated from CV-measurements performed after a pn-junction was formed in the InGaAsSb layer (see below). It is worth noting that not all samples were tested using CV-measurements. As no intentional and thus controllable doping of InGaAsSb was used in this work, the studied samples could have been doped in a range wider than 2-4x10^{16} cm^{-3}.

The growth of the AlGaAsSb layer is carried out from the growth solution having liquidus composition of gallium (x_{Ga}=0.959), antimony (x_{Sb}=0.013) and aluminium (x_{Al}=0.028). Arsenic is added to this melt from an undoped polycrystalline float GaAs wafer through the partial dissolution of the wafer at the growth temperature. The growth of AlGaAsSb is performed either in the same epitaxial run together with InGaAsSb, or in a separate epitaxial process using an InGaAsSb/GaSb wafer as a substrate. The reason to carry out separate processes is the following. We have found that in some experiments drops of the first melt (In-Ga-As-Sb) were left on the surface of the wafer after its wiping (especially at the edges). These drops when mixed with the second melt (Al-Ga-As-Sb), lead to the local formation of unpredictable melt compositions and hence irreproducible growth. A better reproducibility is achieved when the wafer is removed from the boat after the first layer growth, and the drops (if any) are eliminated. In the case of the separate epitaxies, the above-described procedure of the melt baking is repeated for a Ga-Sb part of the melt prior to growth. Al and GaAs floating wafer are added to the melt after the baking and cooling. The growth is performed at 509°C during a 90-sec long contact of the substrate with the melt resulting in a 2-μm thick $Al_{0.28}Ga_{0.72}As_{0.014}Sb_{0.986}$ layer. AlGaAsSb layers grown without intentional doping are p-type. As we need an n-type layer, some Te-doped GaSb with a doping concentration of 2x10^{18} cm^{-3} was added and partly replaced Ga and Sb in the melt. Fig. 1 shows the carrier concentration in n-type $Al_{0.28}Ga_{0.72}As_{0.014}Sb_{0.986}$ vs. the GaSb:Te amount in the Al-Ga-As-Sb melt. Adding of GaSb:Te into the melt provided an accurate control of the electron concentration down to the n=6-7x10^{16} cm^{-3}.

Diffusion of Zn

Pseudo-closed box diffusion of Zn from the vapour phase was performed into n-AlGaAsSb layers in a H_2 atmosphere purified by a Pd cell. A specially designed graphite boat close to that described in [4] was used. Separated pure Zn and Sb vapor sources were used in more than sufficient quantities to provide the saturation of vapour pressures. The design of the graphite boat ensures the uniformity of the Zn vapor pressure across the wafer surface, and thus the uniformity of the p-AlGaAsSb layer depth.

Fig. 2 shows two as-diffused Zn profiles in $Al_{0.28}Ga_{0.72}As_{0.014}Sb_{0.986}$ obtained by means of a 4-hour diffusion of Zn at 460°C and 470°C. The profiles were measured by Secondary Ion Mass Spectroscopy (SIMS). The part of the profile near the surface has a very high concentration of Zn (about 10^{20} cm^{-3}). This 300 – 400 nm thick "dead" layer (shown hatched in Fig. 2) with a low diffusion length of electrons is removed by means of anodic oxidation and selective oxide etching.

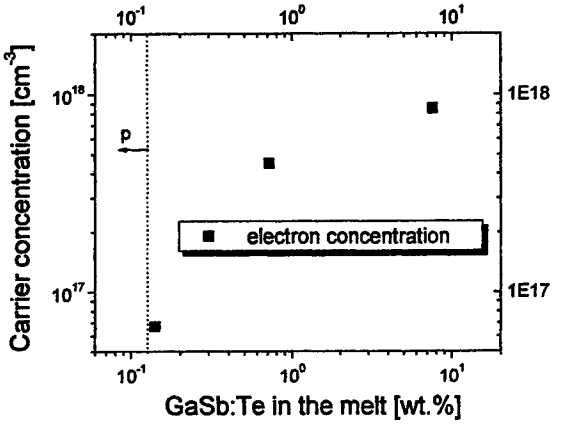

Fig. 1 Carrier concentration in n-$Al_{0.28}Ga_{0.72}As_{0.014}Sb_{0.986}$ layers vs. the amount of tellurium doped GaSb in Al-Ga-As-Sb melt.

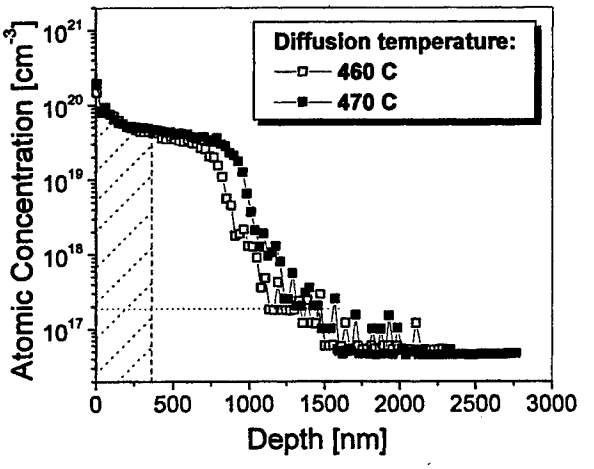

Fig. 2 Zn concentration profiles measured by SIMS in an $Al_{0.28}Ga_{0.72}As_{0.014}Sb_{0.986}$ layer. The hatched part of the profile shows a dead layer that is removed later. The dotted line shows the electron concentration in the n-type $Al_{0.28}Ga_{0.72}As_{0.014}Sb_{0.986}$ layer determined by CV-measurements.

If the AlGaAsSb layer is diffused all the way through, Zn diffusion in InGaAsSb must be considered. To evaluate Zn diffusion in InGaAsSb, data from [5] was used.

Device fabrication

Fig. 3 shows a photodiode mesa structure fabricated and studied in this work. It is composed of a 5-μm thick n-type $In_{0.15}Ga_{0.85}As_{0.17}Sb_{0.83}$ layer with $n=2\text{-}4x10^{16}$ cm^{-3} and a 2-μm thick $Al_{0.28}Ga_{0.72}As_{0.014}Sb_{0.986}$ layer. The n-part of the AlGaAsSb layer is doped at the level of $n=2\text{-}4x10^{16}$ cm^{-3}. In the previous publications of AstroPower [2,3], both p- and n-type AlGaAsSb layers were grown epitaxially. In this work, the p-AlGaAsSb layer was formed by diffusion of Zn from the vapor phase. One can mention the following advantages of this approach:

- Technically, diffusion is simpler than epitaxy
- As only one AlGaAsSb layer is epitaxially grown, a difference in chemical composition between matrices of p- and n-layers is ruled out
- Diffusion of Zn is faster at the places of possible crystal defects in the n-AlGaAsSb layer. Thus, electrical isolation of these defects from the pn-junction takes place. Such isolation is not possible in the case of two epitaxial layers.

By fixing the thickness of the n-AlGaAsSb layer and changing position of pn-junction in it, different types of diodes were fabricated. If pn-junction is in AlGaAsSb and far from the AlGaAsSb-InGaAsSb interface, one gets a pn-AlGaAsSb photodiode. The low bandgap of InGaAsSb is not used in this case. Actually, such diodes were not the purpose of this work. If the pn-junction is in AlGaAsSb close to the AlGaAsSb-InGaAsSb interface, a SAM-APD diode is fabricated. And finally, if the whole AlGaAsSb is diffused all the way through, and pn-junction is formed in the InGaAsSb layer, a pn-InGaAsSb photodiode with an AlGaAsSb window is formed. As it was found in this work, some of these pn-InGaAsSb diodes exhibited avalanching characteristics.

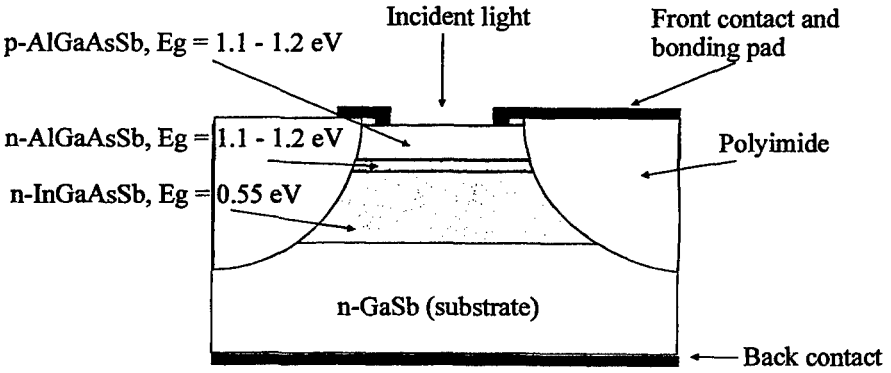

Fig.3 Scheme of the fabricated AlGaAsSb-InGaAsSb SAM-APD. In the case of a pn-InGaAsSb photodiode or APD, the n-AlGaAsSb layer was replaced by a p-InGaAsSb one, and the p-AlGaAsSb layer was used only for the InGaAsSb surface passivation.

Mesa photodiodes with 400-μm diameter total area and 200-μm diameter active area were formed using photolithography and chemical etching (Fig. 4). Metallization for the back n-type contacts was planar Au/Sn while front p-type contacts were annular Ti/Ni/Au A spin-on, photosensitive polyimide

layer was deposited and patterned before contact deposition. This had several functions including planarizing the surface for the front contact deposition, providing insulation of the junction, and passivating the edges of the device area. After photodiodes were formed, the substrate was diced into 1-mm^2 pieces with a single device in the middle of each square. These were mounted to TO-18 headers using silver conducting epoxy and wirebonded from the bonding part of the front contact to the header post. No antireflection coatings were applied.

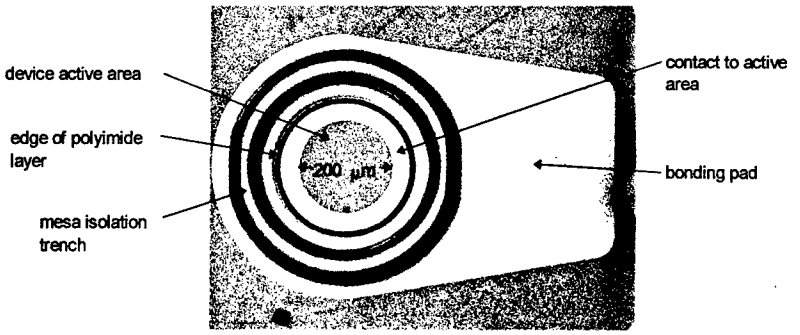

Fig. 4 Top-view of the fabricated photodiodes.

Results and Discussion

Figure 5 shows the comparison of dark I-V curves at room temperature of the best diodes with epitaxial and diffused pn-junctions in the $Al_{0.28}Ga_{0.72}As_{0.014}Sb_{0.986}$ layer. One can see that formation of a diffused pn-junction provides a higher breakdown voltage and essentially lower dark current at the voltages close to the breakdown. This can be explained by the electrical isolation of possible crystal defects in the AlGaAsSb layer due to a higher diffusion rate of Zn in the vicinity of such defects.

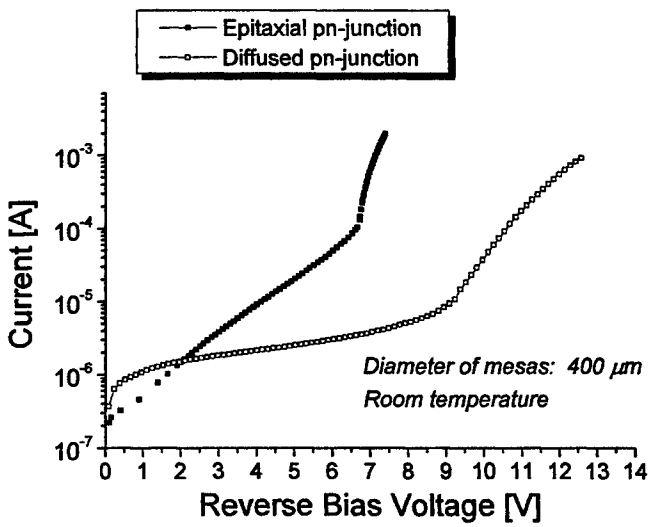

Fig. 5. Dark I-V curves of the best AlGaAsSb/InGaAsSb diodes with epitaxial and diffused pn-junctions in the $Al_{0.28}Ga_{0.72}As_{0.014}Sb_{0.986}$ layer.

Fig. 6 displays dark I-V curves of AlGaAsSb-InGaAsSb diodes with pn-junctions in either AlGaAsSb or InGaAsSb. Samples with pn-junctions in the InGaAsSb layer show quite different behaviors. Two mechanisms of the breakdown are observed: (i) Zener (pn-junction in InGaAsSb of type I), and (ii) avalanching (pn-junction in AlGaAsSb and in InGaAsSb of type II). If avalanching dominates, the breakdown voltage drops with decreasing temperature. Such a behavior was observed in the diode with pn-junction in AlGaAsSb (Fig. 6). The sample with avalanching breakdown of pn-junction in InGaAsSb, in which avalanche multiplication was also determined through responsivity measurements (see Fig.9), have not been measured at low temperature yet. However, one can expect the same positive temperature dependence of the breakdown voltage as it is observed in diodes with pn-junction in AlGaAsSb.

The large difference in IV-curves observed in two types of InGaAsSb samples can be explained by a difference in the n-InGaAsSb doping. As it was mentioned above, the range of doping in InGaAsSb might be wider than 2-4x10^{16} cm^{-3} if no intentional doping is used. Thus a relatively large difference in the width of the space charge region might determine the type of dominating breakdown mechanism: Zener or avalanching.

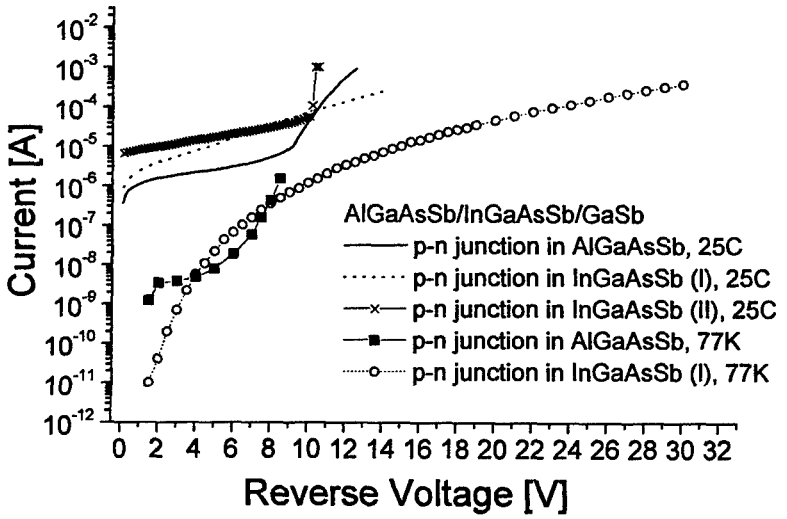

Fig. 6 I-V curves of the AlGaAsSb-InGaAsSb diodes with pn- junctions in different materials at 25°C and 77K. InGaAsSb (I) and InGaAsSb (II) correspond to devices with Zener or avalanching breakdown mechanisms, respectively.

Additional proof of avalanching is provided by spectral response measurements and calculation of quantum efficiency (QE). The only physical reason for the external QE to be higher than 100% is internal amplification caused by the avalanche carrier multiplication.

A computer-controlled spectrometer was used to measure spectral response of the fabricated devices (Fig. 7). The light source is a 1000 W tungsten halogen lamp. A calibrated detector with a calcium fluoride window is used as a reference for relative measurements. This detector has flat response in the wavelength range from 200 nm to over 10 μm. To determine the absolute spectral response, a JPL-calibrated AlGaAsSb-InGaAsSb photodiode with the same design as the tested diodes is used. Additionally, the spectral response of several photodiodes was measured at JPL at 77K.

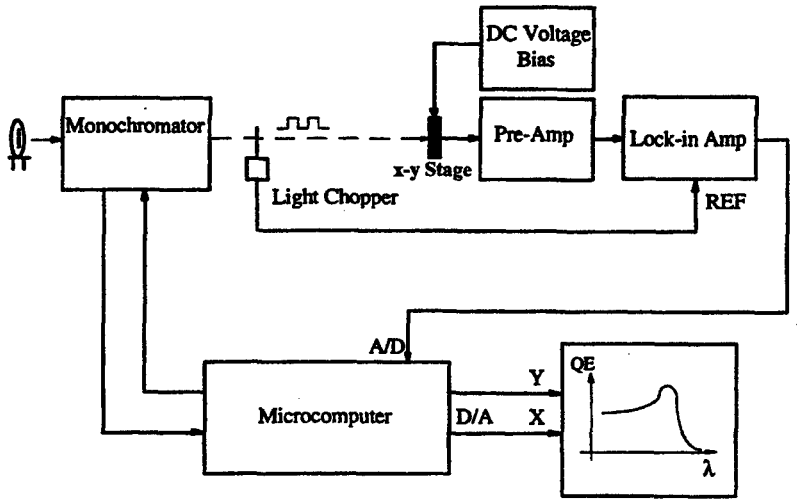

Fig. 7 Spectral response measurement set-up.

Fig.8 shows external QE of an InGaAsSb photodiode with Zener breakdown. Measurements were performed at different reverse biases at 25°C and 77K. A small improvement of the QE is observed after applying the reverse bias up to 3 V. However, there was no further improvement at higher voltages (up to 24V) showing that no avalanche multiplication happened in this diode. The maximum of QE at 77K is shifted to shorter wavelengths due to the increase of the bandgap in InGaAsSb. QE at 77K and at 0 V is lower than at 25°C. However, contrary to the measurements at 25°C, applying reverse voltages at 77K essentially increases QE, and already at 3 V the maximum QE at both temperatures are equal.

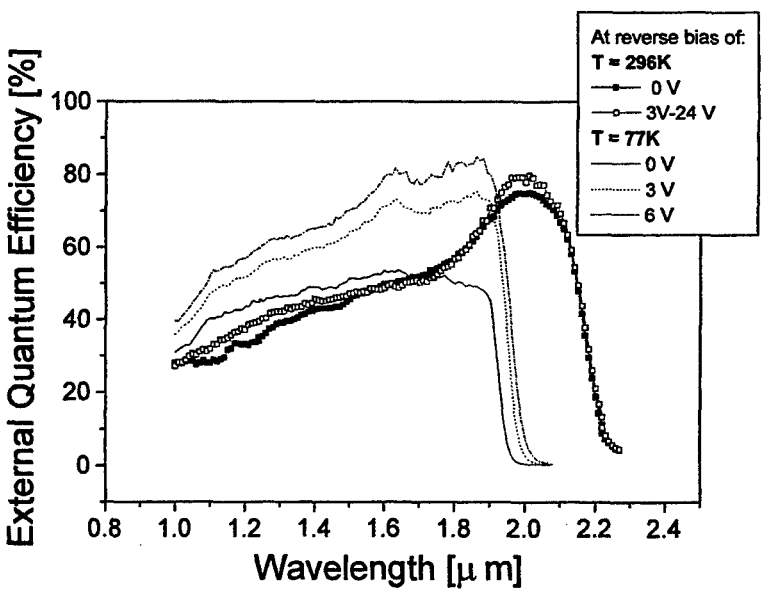

Fig. 8 External quantum efficiency of an InGaAsSb pn-photodiode with the Zener breakdown of pn-junction. Measurements are performed at different reverse biases at 25°C and 77K.

Fig. 9 shows the responsivity of an avalanching InGaAsSb pn-photodiode. Both the IV-curve of this diode with a sharp increase of current at the breakdown voltage (Fig.6), and responsivity vs. reverse voltage (Fig.9) clearly show that this diode is an APD. Improvement of carrier collection and separation due to expanding of the space charge region (SCR) with voltage cannot explain the growth of responsivity up to 3.5 A/W. This value corresponds to an external quantum efficiency of 215 % that is not achievable without the avalanche multiplication. It is noteworthy, that Fig. 9 shows three phases in the dependence of responsivity on reverse bias. The first one is between 0 V and 1 V, when a fast increase of responsivity from 1.2 A/W to 1.6 A/W is observed. The improved collection and separation due to enlarging SCR can explain this increase. The second phase between 1V and 5V is characterized by a saturation of the responsivity increase. Finally, the third phase between 6 V and 8 V shows the avalanche multiplication.

Thus, a low-voltage avalanching regime (starting from 6 V) is achieved in InGaAsSb APDs with an AlGaAsSb window layer. As these diodes demonstrate high responsivity at zero voltage (1.2 A/W), 3.5 A/W responsivity is achieved already at 8 V what we believe is the best result for the wavelength of 2 μm.

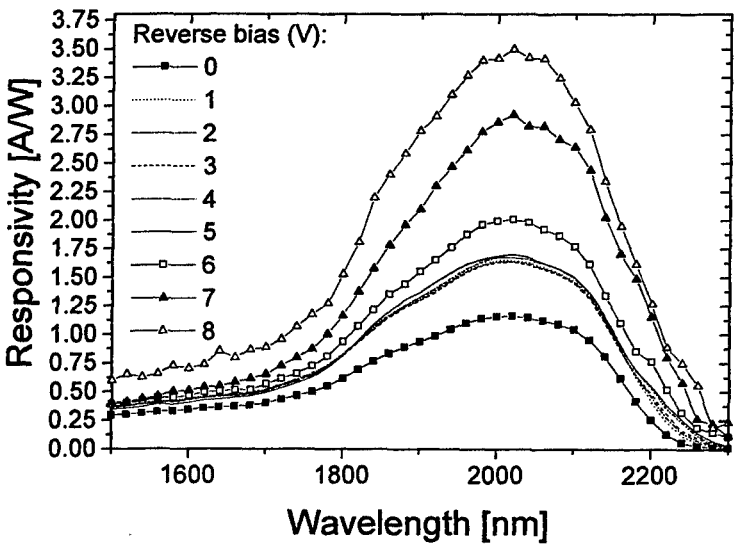

Fig. 9 Spectral response of the low-voltage InGaAsSb APD at different reverse bias voltages. Avalanche multiplication starts at 6 V.

Also, we performed calculations of NEP and D* based on the measured parameters.

The following formula can be derived for *NEP*:

$$NEP = \frac{2qRB + ((2qRB)^2 + 8R^2 qI_d B)^{0.5}}{2R^2},$$

where R is responsivity, I_d is dark current , B is bandwidth, and q is electron charge.

Then

$$D^* = \frac{\sqrt{A} \cdot \sqrt{B}}{NEP},$$

where A is active area of the diode.

Considering the following parameters for the low-voltage InGaAsSb APD at reverse bias of 8V: R = 3.5 A/W (Fig.9), I_d=3x10^{-5}A (Fig.6), A = 3x10^{-4} cm^2 (diameter of photoactive area of 200 μm), and B = 1 Hz, NEP can be calculated as 1x10^{-12} W and D^* value as 2x10^{10} cm·Hz$^{1/2}$/W.

Conclusions

Three different types of heteroface AlGaAsSb/InGaAsSb/GaSb photodiodes are fabricated and studied by using of inexpensive liquid phase epitaxy and diffusion of Zn from the vapor phase.

Both avalanching and Zener breakdown mechanisms are determined in InGaAsSb pn-junctions. This difference can be explained by doping variations of base n-InGaAsSb layers. Controllable rather than unintentional doping must be introduced to provide a more reproducible low doping level of InGaAsSb. Similar to AlGaAsSb doping, it can be done by using GaSb:Te added to the melt as a dopant source.

Low-voltage avalanching regime (starting from 6 V) is achieved in InGaAsSb APDs with an AlGaAsSb window layer. As these diodes demonstrate high responsivity at zero voltage (1.2 A/W), 3.5 A/W responsivity is achieved already at 8 V what we believe is the best result for the wavelength of 2 μm.

An NEP value as low as 1x10^{-12} W or D* value as high as 2x10^{10} cm·Hz$^{1/2}$/W at room temperature is calculated for low-voltage APD diodes with a diameter of photoactive area of 200 μm.

Acknowledgements

The authors wish to thank B. Ber from Ioffe Institute, St. Petersburg, Russia for SIMS measurements and P. Sims from AstroPower for useful discussions.

References

[1] Z.A. Shellenbarger, M.G. Mauk, J.A. Cox, J.D. South, J.D. Lesko, J.R. Bower, P.E. Sims, M.Jhabvala, and M. Kraut Fortin, "Recent progress in GaInAsSb and InAsSbP photodetectors for mid-infrared wavelengths", Proceedings of SPIE, v.3287, pp.138-145 (1998)

[2] Z.A. Shellenbarger, M.G. Mauk, P.E. Sims, J.A. Cox, J.D. Lesko, J.R. Bower, J.D. South, and L.C. DiNetta, " Progress on GaInAsSb and InAsSbP photodetectors for mid-infrared wavelengths", Mat. Res. Soc. Symp. Proc., v. 484, pp. 135-140 (1998)

[3] Z.A. Shellenbarger, M.G. Mauk, M.I Gottfried, J.D. Lesko, and L.C. DiNetta "GaInAsSb and InAsSbP photodetectors for mid-infrared wavelengths", Proceedings of SPIE, v. 2999, pp. 25-33 (1997)

[4] A.W. Bett, S.Keser, and O.V. Sulima, "Study of Zn diffusion into GaSb from the vapour and liquid phase", J. of Cryst. Growth, v. 181, pp. 9-16 (1997)

[5] O.V. Sulima, R. Beckert, A.W. Bett, J.A. Cox, and M.G. Mauk, "InGaAsSb photovoltaic cells with enhanced open-circuit voltage", IEE Proc.-Optoelectron., v. 147, pp. 199-204 (2000)